Nanoscale Res Lett (2010) 5:1449–1455
DOI 10.1007/s11671-010-9660-8

NANO EXPRESS

Fabrication and Properties of Ag-nanoparticles Embedded Amorphous Carbon Nanowire/CNT Heterostructures

Ke-fan Chen · Jian-hua Deng · Fei Zhao · Guo-an Cheng · Rui-ting Zheng

Received: 22 April 2010 / Accepted: 24 May 2010 / Published online: 9 June 2010

Abstract Carbon nanotubes were subjected to doping with an energetic Ag ion beam, and the carbon nanotubes on the top of the array were transformed into amorphous carbon nanowires with embedded Ag-nanoparticles. The field emission characteristics of these nanowires were investigated. The minimum turn-on and threshold fields were 0.68 and 1.09 V/μm, respectively, which were lower than those of the as-grown carbon nanotubes. This was probably because Ag-nanoparticles embedded in the carbon nanowires reduced the effective work function from 4.59 to 4.23 eV. Large doping amounts produced serious structural damage at the top of the nanowires and impaired the field emission characteristics.

Keywords Carbon nanotube · Nanowire · Ion implantation · Field emission

Introduction

Since Iijima's landmark paper on carbon nanotubes (CNTs) in 1991 [1], there has been much research on their fabrications [2, 3], excellent physical and chemical characteristics [4, 5] and potential applications [6]. Rinzler et al. [7] first reported the field emission characteristics of a single multi-walled CNT and pointed out that they have a very low threshold field (E_{th}, which is a applied field at field emission current density of 10 mA/cm^2) and high-field emission current density. The reports of Cheng and Zhou [8] showed that electrons are emitted from the top of CNTs.

Field emission characteristics associated with the structures (composition, tip sharpness, aspect ratio, etc.) and electrical parameters (conductivity, work function, etc.) of emitters. Element doping changes the composition and phase structures of CNTs and improves the field emission characteristics of CNT emitters. CNT arrays doped with boron [9, 10], nitrogen [11] and silicon [12] have been synthesized. Nitrogen-doped CNT arrays have a low turn-on field (1.60 V/μm, E_{on}, which is an applied field at field emission current density of 10 μA/cm^2) and high density of emission points [13]. Liu et al. [14] reported that the gallium doping of CNTs induced the formation of new states near the Fermi level and reduced the work function and enhanced the field emission current density. Some reports [15] have shown that Cs-doped single-walled CNTs have a lower work function and higher field emission current density. Other reports [16] have shown that titanium–carbon compounds synthesized by deposition of titanium films onto the surface of CNTs reduced their work function and improved their field emission characteristics. Previous efforts have attempted to enhance the field emission characteristics of CNTs.

Energetic ion implantation technologies have been widely used to manufacture the semiconductor devices and in many fundamental researches of materials due to their excellent advantages on accurate controllability, superfine processing and no thermal limitation during element doping. Ion implantation of materials leads to defect creation (substitution, interstitial and vacancies creation), doping, re-crystallization and other interesting phenomena, depending on the ion beam parameters such as ion influence and the energy loss of ions in materials.

K. Chen · J. Deng · F. Zhao · G. Cheng (✉) · R. Zheng
Key Laboratory of Beam Technology and Material Modification of Ministry of Education, College of Nuclear Science and Technology, Beijing Normal University, 100875 Beijing, People's Republic of China
e-mail: gacheng@bnu.edu.cn

Recent reports, such as the phase transformation from carbon onion to diamond, the synthesis of CNTs [17], modification of the electronic structure of semiconducting single-walled CNTs [18], synthesis of Zn:C solid solution nanowire/CNT heterostructures [19] and structural damages in nanomaterials [20, 21], have stimulated renewed interests in energetic ion beam fabricated nanomaterials systems and show that energetic ion beam technology is known as a valuable and innovative tool for engineering, synthesis of new nanostructural materials and modification of nanomaterials on molecular or atomic scale. The structure transformation between nanowires and nanotubes has been widely studied [22], and can be induced by chemical reaction [23], surface etching [24] and phase transformation [25].

In this paper, an energetic Ag ion beam process is used to fabricate amorphous carbon nanowires (CNWs) embedded with Ag-nanoparticles to improve the field emission characteristics of the CNWs.

Experimental Details

Fabrication of Amorphous Carbon Nanowires

CNT arrays with high density and good orientation were synthesized on (100) silicon substrates with a thermal chemical vapor deposition method at 750°C for 30 min. During the synthesis of CNT arrays at ambient pressure, a Fe thin film with a thickness of 5 nm, which was prepared by using magnetron sputtering method, was used as a catalyst, and the mixing of hydrogen and acetylene with a H_2/C_2H_2 flow rate ratio of 6.9:1 was used as reactive sources. Energetic ion doping was carried out by using the metal vapor vacuum arc ion implanter [26]. The incidence angle of the ion was about 45°, and the average energy of Ag ions was about 70 keV. The Ag-doped doses ranged from 1×10^{16} to 1×10^{17} cm^{-2}. A TRIM simulation program was used to analyze ion radiation damage of CNTs.

Characterization of Structures and Properties

Scanning electron microscopy (SEM, JSM-4800), high-resolution transmission electron microscopy (HRTEM, TECNAI F30), X-ray photoelectron spectroscopy (XPS, PHI Quantera SXM) and field emission measurement system were employed to characterize morphology, chemical structure and the field emission characteristics of CNTs. The field emission measurements of samples with areas from 0.03 to 0.10 cm^2 were carried out in a bipolar measurement equipment with a measurement distance of about 2,362 μm at room temperature and a base pressure in the chamber is about 1×10^{-7} Pa. The measurement data were automatically recorded by a computer connected to the measurement system.

Results and Discussion

Energetic ion implantation in materials can cause defect creation, doping and re-crystallization. These induce the transformation of composition and phase structure in the target. For one dimension materials, defect creation, doping and re-crystallization will occur in a confined area. Figure 1 shows the microstructure images of CNT arrays doped by energetic Ag ions with different doses. From the cross-section images shown in Fig. 1a–c, the well-aligned nanostructures have been observed in the energetic Ag ion-doped CNT (AD-CNT) arrays and as-grown CNT array. Energetic ion implantation processing dose not destroy the aligned structures of nanoarrays. However, from the top-view images shown in Fig. 1d–f, the top morphologies of nanoarrays show that some differences can be observed. When the doped dose was less than 3×10^{16} cm^{-2}, the morphology at the top of the AD-CNT arrays did not change appreciably (seen in Fig. 1d, e). With further increases in the Ag-doping amount, energy deposition gradually increased and produced serious structural damage on the tip of the AD-CNT arrays. When the doped dose was larger than 6×10^{16} cm^{-2}, the individual nanostructures on the tip of the aligned array gradually disappeared and transformed into net structures (seen in Fig. 1f). It reveals that high doped doses induce serious structural damage at the tip of nanoarrays.

In order to further understand the structural changes occurred in the AD-CNTs, HRTEM was used to determine the crystalline structures of the AD-CNTs. Figure 2 shows HRTEM images of CNTs doped by energetic Ag ions at a dose of 3×10^{16} cm^{-2}. As seen in the TEM image (Fig. 2a), two kinds of structure had been obtained, i.e., nanowire structures at the top and nanotube structures at the bottom of the AD-CNTs. In the part of nanowire, the substrate was amorphous carbon, and many nanoparticles with a size of several nanometers and crystalline structure distribute uniformly in the amorphous carbon substrate (Fig. 2b). These indicated that the amorphous carbon nanowires with embedded nanoparticles have been fabricated at the top of nanoarrays after energetic Ag ion implantation. Calculations of atomic plane separation and angle between two different planes shown in Fig. 2b demonstrated that the particles were metal Ag grains. However, CNT structures with multi-layered graphite remained in the part which was not doped with Ag ions (Fig. 2c). Two different nanostructures existed in a single one dimensional nanomaterial demonstrated the formation

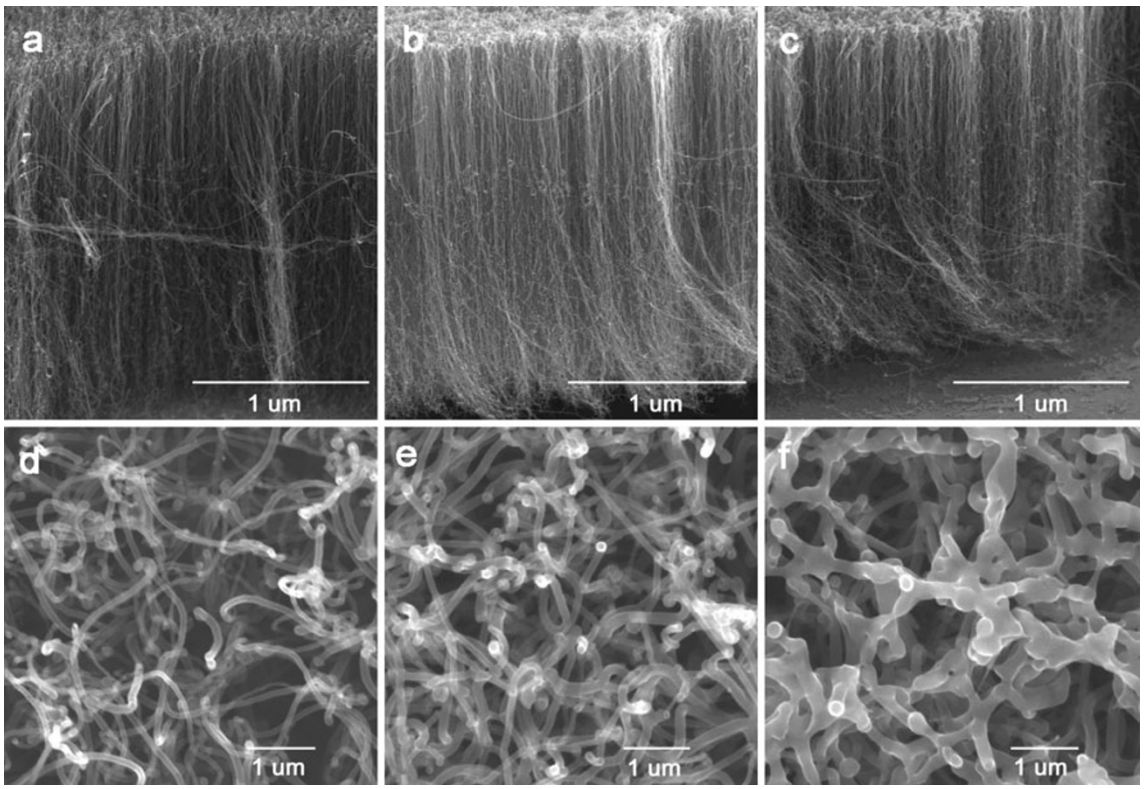

Fig. 1 SEM images of CNTs doped by energetic Ag ions at different doses; **a** Cross-sectional image of as-grown CNT array; **b** Cross-sectional image of the nanoarray doped at 3×10^{16} cm^{-2}; **c** Cross-sectional image of the nanoarray doped at 1×10^{17} cm^{-2}; **d–f** are the top morphologies corresponding to samples in **a**, **b** and **c**, respectively. These cross-sectional SEM images of the nanoarray show well-aligned structures before and after ion implantation. Ag ion implantation with lower dose induces lot of changes in the top microstructures of nanoarrays. However, high-dose ion implantation makes carbon nanonet to be formed

of the Ag-nanoparticle embedded (ANPE) amorphous CNW/CNT hetero nanostructures in the AD-CNTs.

The displacement per atom (dpa) induced by ion radiation is a key parameter of structural damage rate in the target. For energetic Ag ion doping into CNTs, first, the average displacement of carbon atom per implanting ion was calculated using the TRIM simulation program, and second, the dpa of the carbon atom in CNTs doped with different doses were determined using the following formula:

$$dpa = \frac{\Phi \cdot N_1}{N \cdot L} \quad (1)$$

where Φ is the ion-doping dose (ions.cm^{-2}), N is the atomic density (atoms/cm^3) of the target, L is the mean incidence depth of the energetic ion (cm), and N_1 is average dpa of carbon per implanting ion. Table 1 lists the dpa of carbon atom in the CNTs doped by the energetic Ag ion at different doses. The calculated dpa is less than 1.00 when the doped dose is lower than 3×10^{16} cm^{-2}. This means that the energetic Ag ion radiation damage is relatively small in the AD-CNTs. However, the dpa is larger than 1.00, which indicates serious structural damage had occurred in the AD-CNTs when the doses were more than 6×10^{16} cm^{-2}. These results are in agreement with the SEM analysis.

In order to understand chemical structures in the complex nanowires, XPS was used to determine the chemical bonds of Ag and C. Figure 3 shows XPS spectra of the AD-CNTs, in which C1 s peaks and Ag3d5 peaks were clearly observed. Comparing the C1 s peak of as-grown CNTs and the AD-CNTs with a dose of 3×10^{16} cm^{-2}, the peak positions do not change, and only the intensity decrease in peak has been observed due to Ag ion doping. To analyze the C1 s spectrum of the AD-CNTs with a dose of 3×10^{16} cm^{-2} in details, the C1 s peak was fitted by a Gaussian function with three components centered at 284.1, 285.9 and 288.0 eV, respectively. These components corresponded to graphite carbon [27] and organic carbon adsorbed [28, 29]. Peaks centered at 368.2 eV in the XPS spectra were attributed to the Ag3d5 band and corresponded to elemental Ag [30] (Fig. 3b). The Ag-nanoparticles in the amorphous CNWs therefore appeared to be composed of metal Ag instead of Ag-C compound. At the same time, the intensity of the Ag3d5 peaks increased with increases in the Ag-doped doses. The content of metal Ag,

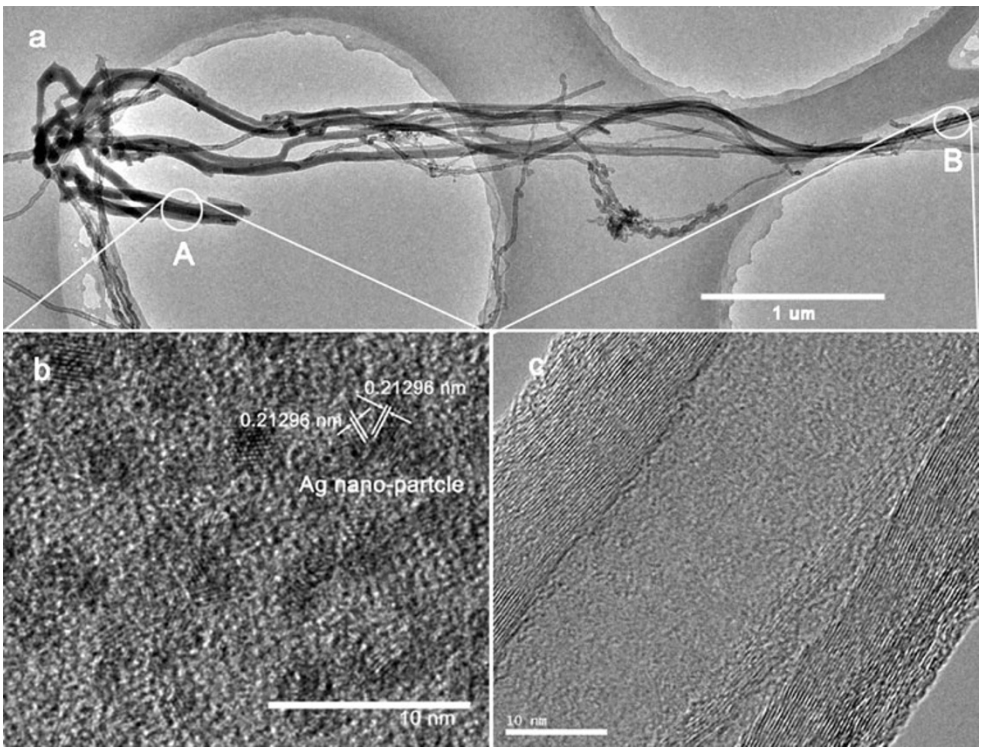

Fig. 2 TEM images of CNTs doped by energetic Ag ions at a dose of 3×10^{16} cm^{-2}; **a** TEM image of CNTs doped by energetic Ag ions, in which two different structures, i.e. nanowire and nanotube, have been observed, it demonstrates that the CNW/CNT hetero nanostructures have been formed in the nanoarray; **b** HRTEM image of A region in image (**a**), which shows the Ag nanoparticles embedded in the amorphous carbon substrate; **c** HRTEM image of B region in image (**a**), which shows CNT structures clearly

Table 1 The calculated dpa of carbon atom in CNTs induced by Ag ion irradiation with different doses

Dose (cm^{-2})	1×10^{16}	3×10^{16}	6×10^{16}	1×10^{17}
dpa (displacement per atom)	0.18	0.55	1.11	1.85

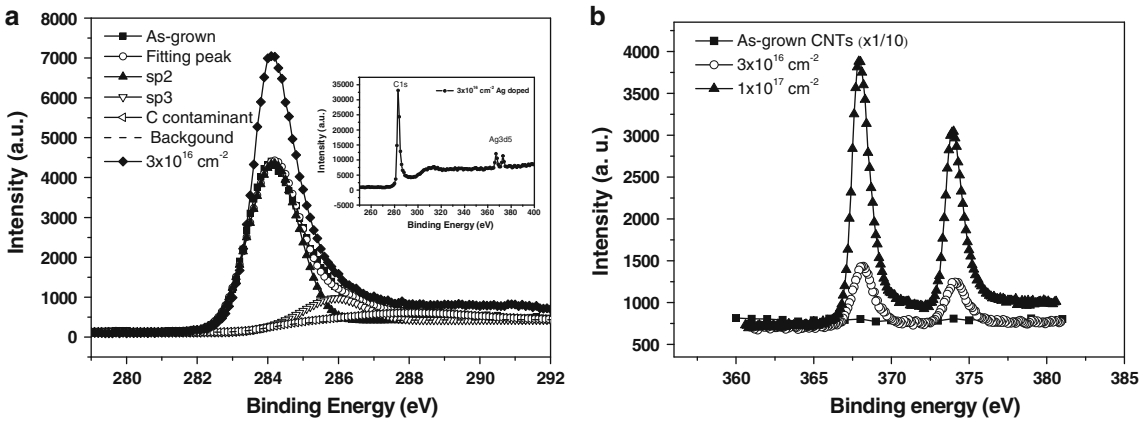

Fig. 3 XPS spectra of energetic Ag-doped CNTs at different doses; **a** C1 s peaks of as-grown CNTs and the CNTs doped at 3×10^{16} cm^{-2}, *inset* is XPS spectrum of CNTs doped at 3×10^{16} cm^{-2}; in which element Ag has been doped into CNTs successively, and the positions of C1 s peaks do not change after Ag ion implantation; **b** Ag 3d5 peaks of CNTs doped at different doses, which demonstrates that the chemical structures of element Ag doped into CNTs are metal Ag instead of C–Ag compound

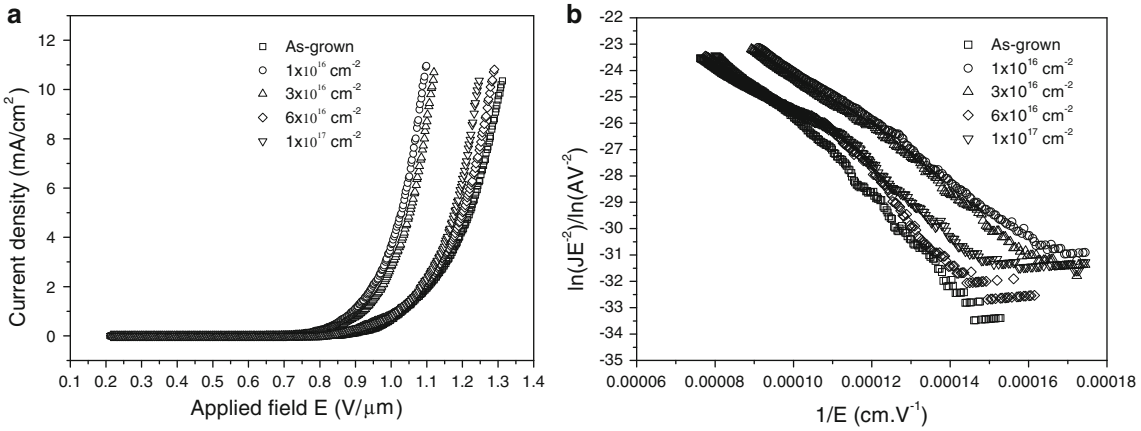

Fig. 4 **a** *J–E* curves of CNTs doped at different Ag ion doses; **b** F–N plots of CNTs doped with different Ag ion doses. The *J–E* curves gradually shift to low applied fields and showed that the field emission characteristics of the AD-CNT arrays were gradually improved as the Ag-doped dose increased from 0 to 3×10^{16} cm^{-2}. Ag ion implantation with high doses makes the field electron emission performance of the emitters worsen

the density and the size of the Ag-nanoparticles in the amorphous CNWs increased with increases in the Ag-doping doses.

Figure 4 shows the curves of emission current density versus the applied field (*J–E* curves) and Fowler–Nordheim (F–N) plots of the CNT arrays doped at different doses. For the field emission characteristics of the AD-CNT arrays, the *J–E* curves indicate typical field emission characteristics and alternately change with the Ag-doped doses. The *J–E* curve first gradually shifted to low applied fields and showed that the field emission characteristics of the AD-CNT arrays were gradually improved as the Ag-doped dose increased from 0 to 3×10^{16} cm^{-2}. However, the *J–E* curve inverted to a right shift or a high applied field. Those indicated that the field emission characteristics of the AD-CNT arrays were gradually reduced when the Ag-doped dose increased from 6×10^{16} to 1×10^{17} cm^{-2}. The F–N plots of the AD-CNT arrays showed an approximately linear relationships between $\ln(J/E_2)$ and $1/E$ in the high applied field area (seen Fig. 4b). This further demonstrated that emission electrons in the *J–E* curves were induced by the applied field.

E_{on} and E_{th} of an emitter are important field emission parameters. Figure 5 shows the E_{on} and E_{th} of the CNT arrays doped at different Ag ion doses. From Fig. 5, the E_{on} and E_{th} of the AD-CNT arrays can be seen to first gradually decrease with the increase in ion dose from 0 to 3×10^{16} cm^{-2} and then to increase with further increases in ion dose. The minimum E_{on} and E_{th} of samples which were doped with a dose of 1×10^{16} cm^{-2} are about 0.68 and 1.09 V/μm, respectively, which are lower than those of the as-grown CNT arrays (E_{on}, 0.80 V/μm and E_{th}, 1.307 V/μm). Comparing the E_{on} and E_{th} of samples doped with 1×10^{16} and 3×10^{16} cm^{-2}, the differences are only about 0.01 and 0.03 V/μm, respectively, and less than 3%.

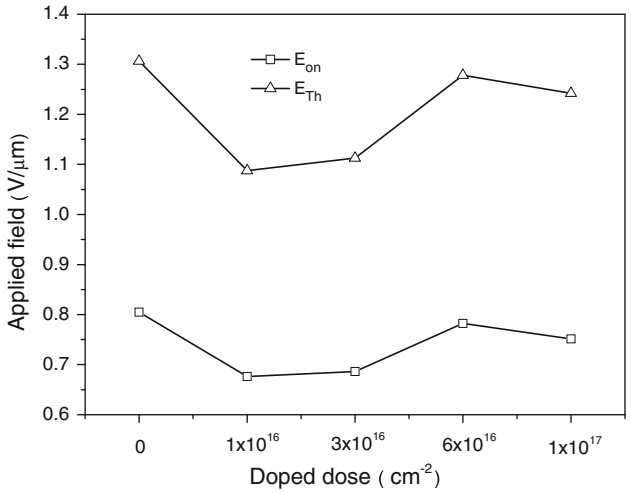

Fig. 5 E_{on} and E_{th} of field electron emission in CNTs versus the doped doses of energetic Ag ions. The E_{on} and E_{th} of the AD-CNT arrays, first, gradually decrease with the increase in ion dose from 0 to 3×10^{16} cm^{-2} and then increase with further increases in ion dose. The minimum E_{on} and E_{th} are about 0.68 and 1.09 V/μm, respectively, which are lower than those of the as-grown CNT arrays

It reveals that the doped dose for the excellent field emission characteristics in the AD-CNT array is in the range from 1×10^{16} to 3×10^{16} cm^{-2}. At the same time, the experimental data show that the field emission characteristics of CNT arrays can be substantially improved and that lower E_{on} and E_{th} values can be obtained using energetic Ag ion processing.

During the energetic Ag ions implantation, the implanted Ag ions triggered a series of atomic collisions among the implanted Ag ions and the target C atoms. According to atomic collision theory, such a process is usually divided into two steps, i.e., atom collision and a relaxation immediately after atom collision, which lasts for a very short

time period of 10^{-10}–10^{-9} s. In the first step, the high energy Ag ions were dynamically launched into the carbon lattice in CNTs where they simultaneously triggered dramatic atom collisions between Ag and C atoms, resulting in the dislocation of C atoms and the formation of a highly energetic Ag and C mixture. It is commonly recognized that, during this step, a lot of defects (substitution, interstitial and vacancies) can be created to induce the formation of disordering distribution of C atoms or amorphous carbon, and the Ag-nanoparticles cannot be formed because these atoms are in violent motion. In the second step of relaxation, beginning at the termination of atom collisions, the bombarded but not moved carbon atoms would vibrate in the solid target. If the energy is released in the form of thermal energy, a global thermal spike centered at the thermal source would be formed. According to the calculation of literature [12], if the vibrational energy is completely transformed into thermal energy, the temperature of the globe with a diameter of 10 Å increases to more than 1,000°C. In our experiment, the Ag atoms cannot be miscible into carbon structures because of immiscibility between Ag and C, which made it possible that the Ag atoms diffused in carbon nanostructures to form Ag atom cluster instead of Ag–C compound. On the other hand, the implantation of high-energy Ag ions into CNTs induced high-density defects, especially vacancies. These vacancies enhance the diffusion of Ag atoms to form Ag-nanoparticles in carbon structures. Thus, the ANPE-CNW can be synthesized in the Ag ion-doped area of CNTs, and the tubular structures with multi-layered graphite remain in the undoped area of CNTs. Therefore, ANPE-CNW/CNT hetero nanoarrays have been synthesized by the energetic Ag ion-doping process. We assume that the field enhancement factor β of the Ag ion-doped nanoarrays is approximately the same as that of the as-grown CNT arrays, because the morphology changes in the Ag ion-doped nanoarrays are relatively small for the smaller doping amounts. According to the F–N plots in Fig. 3b, the efficient work function φ_{eff} of the ANPE-CNW/CNT nanoarrays can be calculated from the F–N equation [31]. For the ANPE-CNW/CNT nanoarrays, the minimum φ_{eff} is about 4.23 eV and lower than that of CNTs (4.59 eV[32]). This decrease in φ_{eff} is favorable for electron emitting from the top of the nanoarrays and enhances the field emission characteristics of the emitter. This demonstrates that the enhancement of the field emission characteristics of the nanoarrays is due to the formation of the ANPE-CNWs at the top of the nanoarrays.

High-dose implantation will create a lot of dislocation and sputtering of carbon atoms and induce the breakdown of the top microstructure in the nanoarrays due to energetic ion irradiation. According to the calculated data from Table 1, the dpa of carbon atoms is larger than 1.00 when the Ag ion-doped doses are higher than 6×10^{16} cm^{-2}. The large dpa shows that the average displacement of every atom in the doping area of the CNTs from equilibrium lattices occurs more than once and induces serious structural damage at the top of the CNT arrays. Here, the individual structures of nanowires at the top of the nanoarrays have been destroyed and transformed into a carbon nanonet, as demonstrated by SEM analysis. The formation of the carbon nanonet structures at the top of the CNT array decreases the numbers and enlarges the sizes of emitting points. All of these changes worsen the field electron emission performance of the emitters.

Conclusion

Well-aligned ANPE amorphous CNW/CNT hetero nanoarrays based on CNT arrays have been fabricated by energetic ion beam processing with doses from 1×10^{16} to 3×10^{16} cm^{-2}, in which the sizes of Ag grains are only several nanometers. Large doping amounts produce serious structural damage and cause the formation of carbon nanonet structures at the top of the nanoarrays. The formation of ANPE amorphous CNWs at the top of CNTs enhances the field emission characteristics of the CNTs. The φ_{eff}, the minimum E_{on} and E_{th} of the ANPE amorphous CNW/CNT hetero nanostructures are 4.23 eV, 0.68 and 1.09 V/μm, respectively, and these values are lower than those of the as-grown CNTs. Serious structural damage and the formation of carbon nanonet structures occurred at the top of CNT arrays, which impaired the field electron emission characteristics of the emitters.

Acknowledgments This work was supported by National Basic Research Program of China (No: 2010CB832905) and partially by National Natural Science Foundation of China (No: 10575011) and the Key Scientific and Technological Project of Ministry of Education of China (No: 108124).

References

1. S. Iijima, Nature **354**, 56–58 (1991)
2. H.P. Liu, G.A. Cheng, R.T. Zheng, Y. Zhao, C.L. Liang, J. Mol. Catal. A Chem. **247**, 52–57 (2006)
3. H.P. Liu, G.A. Cheng, R.T. Zheng, Y. Zhao, C.L. Liang, Surf. Coat. Technol. **202**, 3157–3163 (2008)
4. S.J. Kang, Y.J. Song, Y.J. Yi, W.M. Choi, S.M. Yoon, J.Y. Choi, Carbon **48**, 520–524 (2010)
5. C. Hierold, A. Jungen, C. Stampfer, T. Helbling, Sens Actuators A **136**, 51–61 (2007)

6. J.W. Kang, Q. Jiang, Nanotechnology **18** doi:10.1088/0957-4484/18/9/095705 (2007)
7. A.G. Rinzler, J.H. Hafner, P. NIkolaev, P. Nordlander, D.T. Colbert, R.E. Smalley, L. Lou, et al., Science **269**, 1550–1553 (1995)
8. Y. Cheng, O. Zhou, C. R. Phys. **4**, 1021–1033 (2003)
9. W.Q. Han, Y. Bando, K. Kurashima, T. Sato, Chem. Phys. Lett. **299**, 368–373 (1999)
10. J. Yu, X.D. Bai, J. Ahn, S.F. Yoon, E.G. Wang, Chem. Phys. Lett. **323**, 529–533 (2000)
11. R.B. Sharma, D.J. Late, D.S. Joag, A. Govindaraj, C.N.R. Rao, Chem. Phys. Lett. **428**, 102–108 (2006)
12. H.P. Liu, G.A. Cheng, C. L. Liang, R.T. Zheng Nanotechnology **19**, 245606 (2008)
13. Y. Chai, L.G. Yu, M.S. Wang, Q.F. Zhang, J.L. Wu, Universitatis. Pekinensis **42**(1), 89–92 (2006)
14. K. Liu, H.Y. Li, Q. Li, E.J. Liang, J. Henan Univ. **36**(4), 24–27 (2006)
15. A. Wadhawan, R.E. Stullcup, J.M. Perez, Appl. Phys. Lett. **78**, 108–110 (2001)
16. Y.X. Qing, M. Hu, Appl. Surf. Sci. **254**, 3313–3317 (2008)
17. A.V. Krasheninnikov, F. Banhart Nat. Mater. **6**, 723–732 (2007)
18. A. Tolvanen, G. Buchs, P. Ruffieux, P. Gröning, O. Gröning, A.V. Krasheninnikov, Phys. Rev. B **79**, 125430 (2009)
19. K.F. Chen, J.H. Deng, F. Zhao, G.A. Cheng, R.T. Zheng, Sci. China Tech. Sci. **53**, 776–781, doi:10.1007/s11431-009-0384-x (2010)
20. A. Kumar, F. Singh, P.M. Koinkar, D.K. Avasthi, J.C. Pivin, M.A. More, Thin Solid Films **517**, 4322–4324 (2009)
21. S. Mathew, U.M. Bhatta, J. Ghatak, B.R. Sekhar, B.N. Dev, Carbon **45**, 2659–2664 (2007)
22. Y. Chenglin, L. Jun, L. Fei, W. Junshu, G. Kun, X. Dongfeng, Nanoscale Res. Lett. **3**, 473–480 (2008)
23. Y. Chenglin, X. Dongfeng, J. Phys. Chem. B **110**, 25850–25855 (2006)
24. Y. Chenglin, X. Dongfeng, Electrochem. Comm. **9**, 1247–1251 (2007)
25. Y. Chenglin, X. Dongfeng, Adv. Mater. **20**, 1055–1058 (2008)
26. T.H. Zhang, Y.G. Wu, Beijing: Science Press of Beijing (1999)
27. R. Bertoncello, A. Casagrande, M. Casarin, A. Glisenti, E. Lanzoni, L. Mirenghi et al., Surf. Interface. Anal. **18**, 525–531 (1992)
28. B. Folkesson, P. Sundverg, R. Larsson, J. Elect. Spectrosc. Relat. Phenom. **46**, 19–29 (1988)
29. D. Rats, J. Sevely, L. Vandenbulcke, R. Benoit, R. Erre, V. Serin, et al., Thin Solid Films **270**, 177–183 (1995)
30. G. K. Wertheim, J.H. Wernick, S. Hufner, Solid State Commun., **17**, 417–422 (1975)
31. R.G. Forbes, Ultramicroscopy **79**, 11–23 (1999)
32. Z.X. Chen, G.C. Cao, Q. Zhang, B.J. Zhu, Z.L. Lin, High Power Laser Part Beams **18**, 2070–2073 (2006)